

Higher Order DSD Calibration of Ammonium Nitrate/Fuel Oil

Carlos Chiquete[†], Mark Short, Scott I. Jackson and John B. Bdzil
Shock and Detonation Physics Group
Los Alamos National Laboratory
Los Alamos, NM USA

1 Introduction

Modern Programmed Burn (PB) strategies for calculation of detonation propagation in high explosives utilize the Detonation Shock Dynamics (DSD) modeling methodology to obtain time-of-arrival information of the surface throughout the geometry of interest [4–6, 9]. Within DSD at “leading order”, the normal detonation velocity is related *only* to the local surface curvature according to a prescribed parameterized function. Given a set of calibration experiments for a particular explosive from simple axisymmetric cylindrical (“rate-stick”) and/or slab geometry tests (described in [7]), the relevant propagation law parameters are typically found from fitting DSD calculations to experimental detonation velocities and front shapes.

Relative to ideal explosives, the leading order DSD theory produces considerably larger fit errors for non-ideal explosives. For the non-ideal 94%/6% by weight Ammonium Nitrate/Fuel Oil (ANFO) mixture, a calibration procedure of a higher order (parabolic) DSD evolution equation was developed to increase fidelity to the experimental rate-stick data by Bdzil *et al.* [3]. This particular form includes the effects of transverse flow and shock acceleration. The HODSD calibration effort was successful in reducing the fit error residuals relative to the conventional $D_n - \kappa$ calibration by Bdzil [2].

Subsequent to these initial DSD and HODSD calibrations, slab geometry tests for ANFO were performed by Jackson & Short [8]. Given these uncalibrated slab tests, the predictive capability of the calibrations derived solely from the rate-stick data can be tested. Figure 1 shows size effect (SE) curves derived from a conventional DSD calibration. The SE denotes the dependence of axial detonation velocity on both charge-thickness and charge-radius. The two curves are evidently too close to match the separation in the experimental SE data when plotted on the inverse charge-radius and charge-thickness axis. However, the higher order DSD calibration performed by Bdzil *et al.* [3] better predicts the slab geometry data (see Figure 2(a)).

Given this predictive success of the HODSD theory relative to the leading order DSD, the HODSD calibration of ANFO was revisited in this work at a lower Chapman-Jouguet value. This was motivated by an analysis of the rate-stick data by Bdzil [2] which suggested that the limiting value should be lowered to improve fit results, specifically from 5.2 to 4.8 mm/ μ s. In the following, the applied HODSD calibration procedure is described and the new calibration results are presented.

[†]Correspondence to: chiquete@lanl.gov

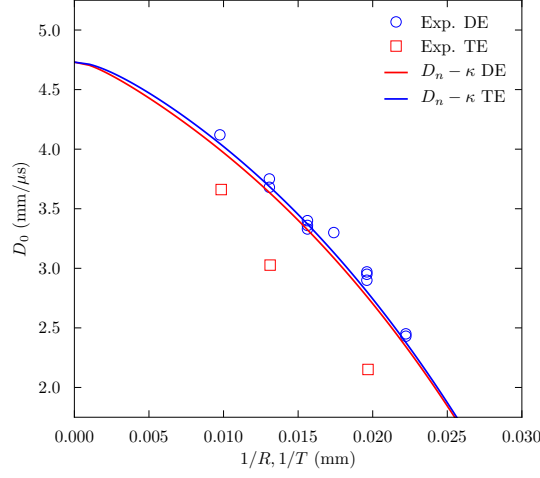


Figure 1: ANFO SE data in symbols and SE solid curves derived from a leading order $D_n - \kappa$ calibration.

2 Implemented higher order calibration

In [1], Aslam *et al.* derived a higher order propagation law with additional asymptotic contributions from both front acceleration and transverse flow to the conventional (leading order) DSD analysis. Bdzil *et al.* [3] adapted this more complex propagation law and used it to calibrate the ANFO rate-stick experimental data set. Specifically,

$$\kappa = F(\mathcal{D}) - A(\mathcal{D}) \frac{D\mathcal{D}}{Dt} + B(\mathcal{D}) \frac{\partial^2 \mathcal{D}}{\partial \xi^2}, \quad (1)$$

where κ is the total surface curvature, D_n is the normal detonation velocity, D_{CJ} is the limiting Chapman-Jouguet velocity for the explosive, and \mathcal{D} was a non-dimensional velocity deficit and related to D_n and D_{CJ} via $\mathcal{D} = D_n/D_{CJ} - 1$. The HODSD prescribed functions were as in [3],

$$A(\mathcal{D}) = A, B(\mathcal{D}) = B, \text{ and } F(\mathcal{D}) = -E_1 \mathcal{D} \exp\left(-\frac{C_1}{\mathcal{D} + 1}\right), \quad (2)$$

where A, B, E_1 and C_1 are fitting parameters. where t_r is the relaxation time to quasi-steady flow for the propagation of the detonation wave. The transverse flow term in (1) includes the second derivative of \mathcal{D} with respect to ξ which denotes the arclength coordinate. The total derivative with respect to t appears in the acceleration term in (1), where $D/Dt = \partial/\partial t + D_n \cdot \partial/\partial n$ and n is the normal direction to the surface. Note that for this particular propagation law model, an approximate analysis of (1) leads to

$$t_r \propto \sqrt{A/D_{CJ}}. \quad (3)$$

DSD calibration experiments are typically performed in simple rate-stick or slab geometries meant to produce quasi-steady flow in the explosive where the axial detonation velocity and detonation front shape are measured. For calibrating the parameters of the higher order propagation law (1), the geometry is reduced to the cylindrical axisymmetric case (or slab geometry) in the quasi-steady state moving at a prescribed axial detonation velocity, D_0 . The front coordinates are obtained from

$$\frac{dr}{d\phi} = \frac{\cos \phi}{\kappa_s}, \quad \frac{dz}{d\phi} = -\frac{\sin \phi}{\kappa_s}, \quad (4)$$

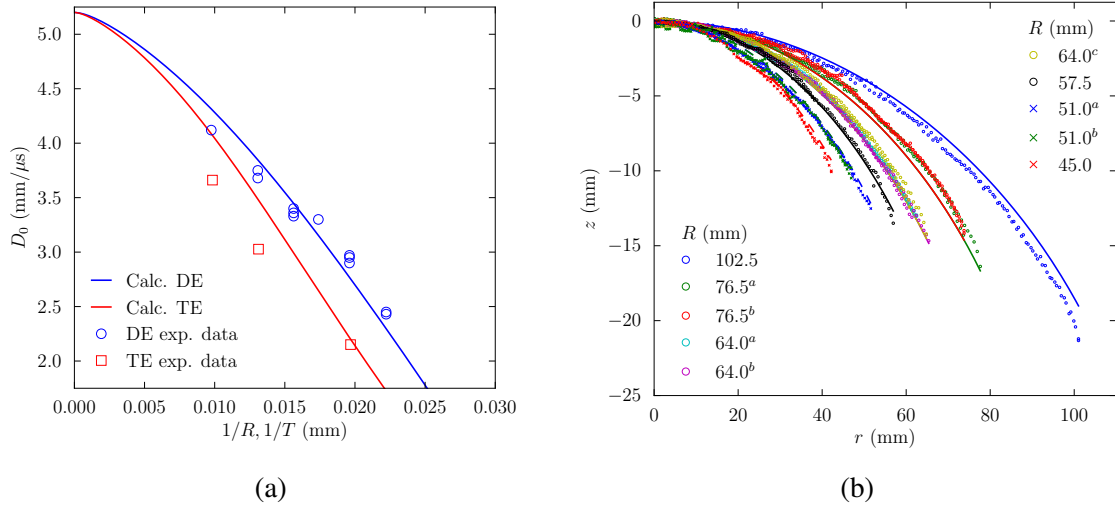


Figure 2: (a) Calculated SE curves compared to the experimental SE data using HODSD calibration obtained by Bdzil *et al.* [3] for $D_{CJ} = 5.2$ mm/ μ s. (b) Calculated front shape comparison to the experimental front shapes.

where r and z are, respectively, the radial and height front shape coordinates in the moving shock frame of reference, ϕ is the shock angle of the surface relative to the axial direction and the slab curvature is denoted by κ_s . In the leading order evolution equation ($\kappa = F(\mathcal{D})$), κ_s is determined from the prescribed relation between κ and D_n , but within HODSD, it is determined from an ordinary differential equation (ODE) for κ_s (1), namely

$$\left(\kappa_s \frac{D_0}{D_{CJ}} \sin \phi \right) \cdot \frac{d\kappa_s}{d\phi} = -\frac{D_0}{D_{CJ}} \kappa_s^2 \cos \phi - \frac{1}{B(\mathcal{D})} \cdot \left(\kappa_s + \alpha \frac{\sin \phi}{r} - F(\mathcal{D}) - D_{CJ} \left(\frac{D_0}{D_{CJ}} \sin \phi \right)^2 \cdot A(\mathcal{D}) \cdot \kappa_s \right). \quad (5)$$

Here the symmetry factor $\alpha = 0$ denotes a slab test geometry and $\alpha = 1$ denotes a rate-stick geometry. The integration begins at a small finite value of $\phi = \phi_0 \ll 1$. The analogue system with r as independent variable can be obtained simply from (4,5) using $d\phi/dr = \kappa_s / \cos(\phi)$.

In addition to the functional parameters A, B, E_1 and C_1 , the parameters necessary for integrating the ODE system include D_{CJ} (mm/ μ s) and the edge angle parameter, ϕ_e , which characterizes the interaction between the confining material and the explosive for each calibration experiment. Laminated, waxed paper (for rate-sticks) or plywood (for slabs) were the confining materials in the relevant ANFO experiments. As a result, it was assumed that there is no effective confinement rendering ϕ_e as the sonic angle. Note that D_{CJ} and ϕ_e radians and were fixed in each in the current calibrations (to 4.8 mm/ μ s and 0.5 radians, respectively). The current calibration procedure minimized a merit or fit error function which was based on the Bdzil form used in [3]. The front shape and detonation velocity errors were considered as different components in the merit function with their relative balance set to slightly promote diameter effect error reduction.

The calibration data set for ANFO was expanded in relation to the Bdzil set. Specifically, two additional rate-stick geometry front shapes at 2 charge-radii (76.5 and 64.0 mm) were used. Note that the additional 3 slab-geometry velocity points at the 3 different charge-thicknesses (101.6, 76.2 and 50.8 mm) were not calibrated. The recent slab experiments performed by Jackson & Short are described in [8].

3 Current calibration results

Figure 3 shows the results of the present work in calibrating the rate-stick data set using the lower $D_{C,J}$ value. It is readily apparent that the calibrated diameter effect curve significantly improves the fit error relative to the previous HODSD calibration. The front shape fit error was also improved. Given that only the rate-stick data was calibrated, the predicted thickness effect curve for the present calibration is significantly closer to the experimental slab velocity data relative to the calibration in [3].

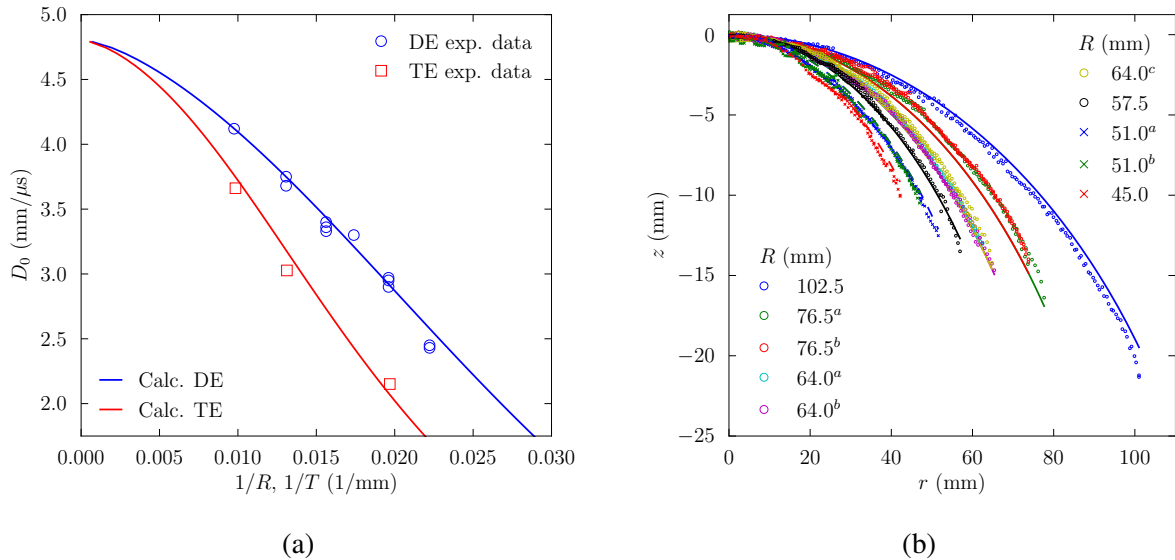


Figure 3: (a) Calculated SE curves compared to the experimental SE data and (b) calculated front shapes compared to the data for the present calibration.

The substantial improvement to the prediction of the thickness effect relative to the leading order DSD theory points to the importance of the additional physical effects incorporated in the HODSD theory for this non-ideal explosive. This is illustrated in Figure 4 via the calculated curvature components in the higher order propagation law for the various charge sizes in the front shape data set. The higher order contributions to the total curvature were considerable throughout each domain. Finally, for this particular set of propagation law parameters, the relaxation time for the present higher order propagation law was found to be consistent with rate-stick experiments in which detonations achieve a quasi-steady state after having propagated an axial distance of a few charge-diameters [3].

References

- [1] T.D. Aslam, J.B. Bdzil, and L.G. Hill. Extensions to DSD theory: Analysis of PBX 9502 rate stick data. In *11th Int. Det. Symp.*, pages 21–29, 1998.
- [2] J. B. Bdzil. Detonation shock dynamics calibration for ANFO. Private communication, 2008.
- [3] J.B. Bdzil, T.D. Aslam, R.A. Catanach, L.G. Hill, and M. Short. DSD front models: nonideal explosive detonation in ANFO. In *12th Int. Det. Symp.*, 2002.
- [4] J.B. Bdzil, W. Fickett, and D.S. Stewart. Detonation shock dynamics: A new approach to modeling multi-dimensional detonation waves. In *9th Int. Det. Symp.*, pages 730–42, 1989.

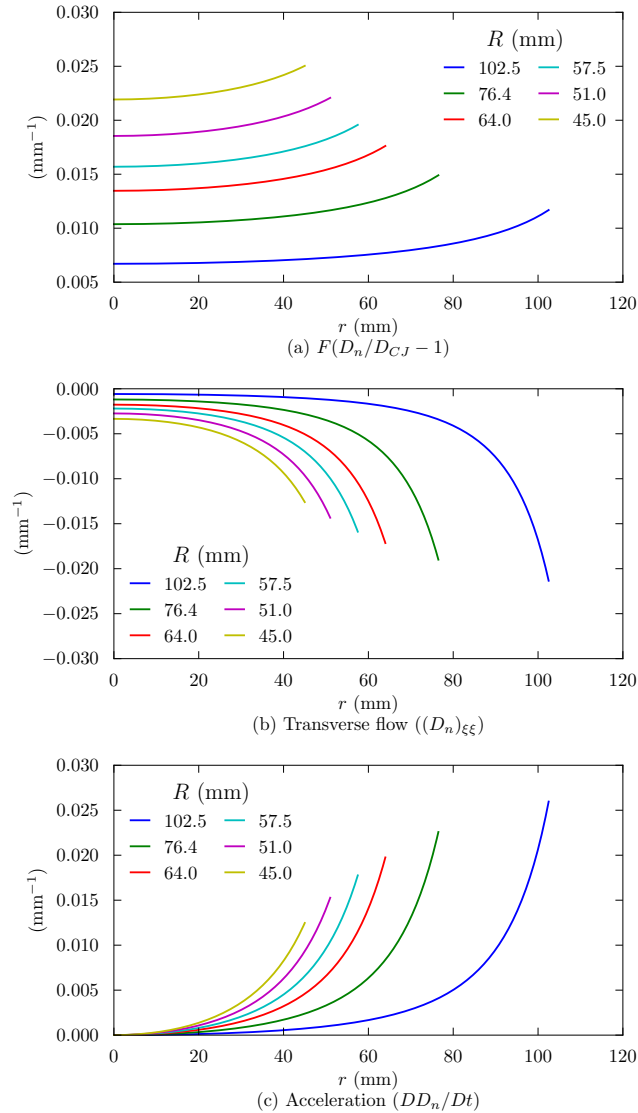


Figure 4: Calculated curvature components as a function of r for each calibrated front shape data set.

- [5] J.B. Bdzil and D.S. Stewart. Modeling two-dimensional detonations with detonation shock dynamics. *Phys. of Fluids A: Fluid Dyn.*, 1:1261, 1989.
- [6] J.B. Bdzil and D.S. Stewart. The dynamics of detonation in explosive systems. *Ann. Rev. Fluid Mech.*, 39:263–292, 2007.
- [7] L.G. Hill and T.D. Aslam. The LANL detonation-confinement test: prototype development and sample results. In *AIP Conf. Proc.*, volume 706, page 847, 2004.
- [8] S.I. Jackson and M. Short. Scaling of detonation velocity in cylinder and slab geometries for ideal, insensitive and non-ideal explosives. *J. Fluid Mech.*, 2015. Submitted.
- [9] D.S. Stewart and J.B. Bdzil. The shock dynamics of stable multidimensional detonation. *Combust. Flame*, 72(3):311–323, 1988.